Geminally Substituted Tris(acenaphthyl) and Bis(acenaphthyl) Arsines, Stibines and Bismuthine: A Structural and NMR Investigation

Brian A. Chalmers, Christina B. E. Meigh, Phillip S. Nejman, Michael Bühl, Tomáš Lébl, J. Derek Woollins, Alexandra M. Z. Slawin, Petr Kilian*

EaStChem School of Chemistry, University of St Andrews, St Andrews, Fife KY16 9ST, UK. Email: pk7@st-andrews.ac.uk

Abstract

Tris(acenaphthyl) and bis(acenaphthyl) substituted pnictogens (*i*Pr_2P-Ace)$_3$E (**2**–**4**) (E = As, Sb, Bi; Ace = acenaphthene-5,6-diyl) and (*i*Pr_2P-Ace)$_2$EPh (**5** and **6**), (E = As, Sb) were synthesised and fully characterised by multinuclear NMR, HRMS, elemental analysis and single crystal X-ray diffraction. The molecules adopt propeller-like geometries with the restricted rotational freedom of the sterically encumbered *i*Pr_2P-Ace groups resulting in distinct NMR features. In the tris(acenaphthyl) species (**2**–**4**) the phosphorus atoms are isochronous in the $^{31}P\{^1H\}$ NMR spectra, and the rotation of the three acenaphthyl moieties around E–C_{ipso} bond is locked. On the other hand, the bis(acenaphthyl) species show a fluxional behaviour, resulting in an AX to A_2 spin system transition in the $^{31}P\{^1H\}$ VT NMR spectra. This allowed elucidation of remarkable through-space couplings of $^{8TS}J_{PP}$ 11.5 Hz (for **5**) and 25.8 Hz (for **6**) at low temperature. In addition, detailed lineshape analysis of the thermodynamic parameters of the restricted rotation of the "propeller blades" in **5** was performed in the intermediate temperature region and also at coalescence. The lone pairs on the pnictogen atoms in **2**–**6** are oriented such that they form a bowl shaped area which is somehow buried within the molecule.

Introduction

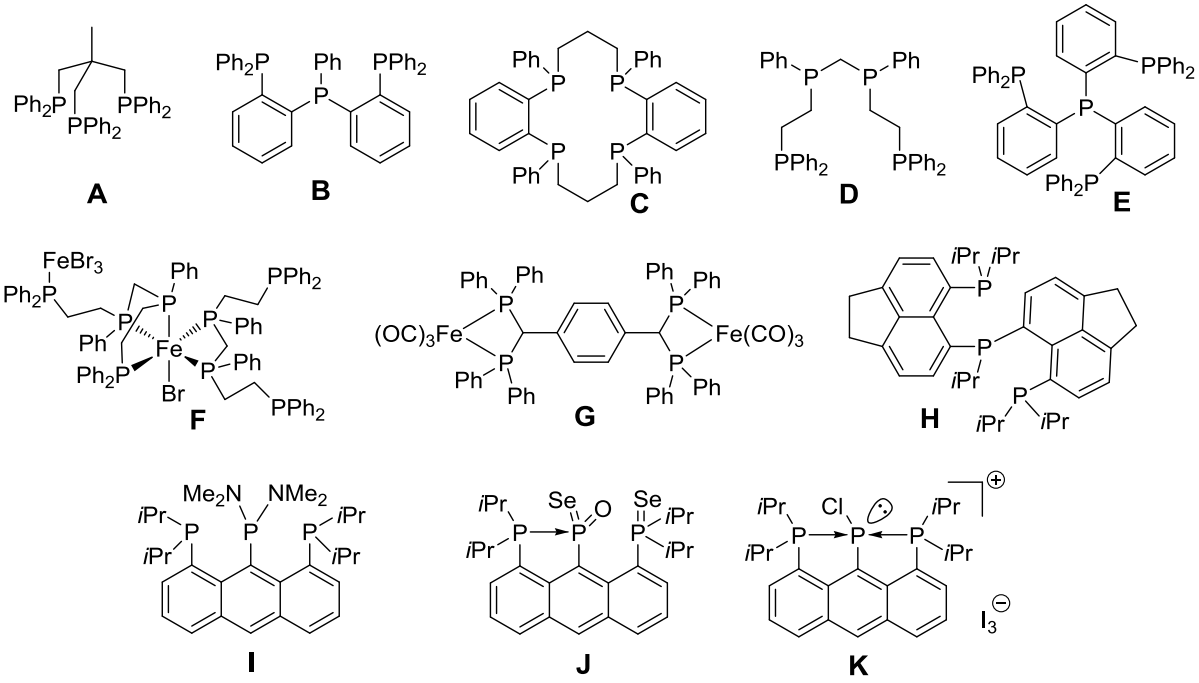

Figure 1: Selected literature examples of tri- and tetradentate phosphines (**A**–**E**), metal complexes (**F**, **G**) and 1,8,9-substituted anthracenes (**I**–**K**) discussed herein.

Tridentate phosphines have been described extensively in the literature, with the majority of reports focussing on their use in catalysis.[1] As for other phosphines, the versatility of tridentate phosphines as ligands stems from the ability to manipulate the steric and electronic properties by varying the groups attached to the phosphorus donor atoms. In addition, flexibility of the linkages joining the donor atoms in multidentate ligands is also tunable. The rather flexible ligand, triphos (**A**), is one of the most extensively studied tridentate phosphines as mentioned in a recent review by Ilia.[2,3] Ligand **B** represents a less flexible tris(phosphines), with o*rtho*-substituted phenyl linkages favouring metal chelation.[4] On the other hand, tetradentate phosphines such as **C** [5], **D** [6] and **E** [4] have been much less explored, often due to the challenging multi-step synthesis involved. Coordination chemistry of these ligands is somehow complicated by the variety of coordination modes these ligands display, which makes their chemistry somehow less predictable. An example of this coordinative variety includes the bimetallic iron(II) complex **F** in which one tetrakis(phosphine) ligand **D** is coordinating in a bidentate mode, and the other in a tridentate mode to one metal atom and monodentate to the other.[6] More rigid tetradentate phosphines also form bimetallic bidentate systems such as complex **G**, which was obtained from the reaction of tetrakis(diphenylphosphino)-*p*-xylene with $Fe_2(CO)_9$.[7]

We have recently reported a synthetic and coordination study of the first geminally bis(*peri*-substituted) tridentate phosphine (**H**).[8] It was synthesised by the reaction of Li–**1** with half an equivalent of *i*PrPCl$_2$, giving the tris(phosphine) in a respectable yield (68%). The tris(phosphine) **H**

displayed complex variable temperature (VT) NMR behaviour. At room temperature a broad singlet was observed in the $^{31}P\{^{1}H\}$ NMR spectrum, which resolved to an AB_2 system at elevated temperature (353 K). Upon cooling to 223 K, two ABC spin systems were observed, due to two rotamers of the compound being present in solution. The complexity of the dynamic processes prevented the extraction of detailed thermodynamic parameters by $^{31}P\{^{1}H\}$ VT NMR spectroscopy. Tris(phosphine) **H** was shown to act as a tridentate ligand forming square planar, tetrahedral, trigonal bipyramidal and octahedral complexes with various metals (Pt, Cu, Fe and Mo).

Tris(phosphine) **H** bears some similarity to 1,8,9-trisubstituted anthracenes, in which the central atom (in position 9) also experiences two proximate *peri*-interactions. We have previously synthesised a short series of tris(phosphino)anthracenes with a particular interest in their *peri*-region bonding and through space interactions.[9] Compound **I** shows no formal P–P bonding interaction, though it does show a remarkable $^{4TS}J_{PP}$ of 104 Hz in an A_2M spin system. The Lewis base stabilised *meta*-phosphonate **(J)** was synthesised from the reaction of **I** with methanol and selenium and the double Lewis-base stabilised phosphenium (**K**) was somehow unexpectedly synthesised by the reaction of **I** with P_2I_4 in 1,2-dichloroethane. Whilst of high interest for their interesting bonding, several aspects make pnictogen 1,8,9-trisubstituted anthracenes rather challenging species to work with. Firstly, six synthetic steps are required in the preparation of **I**, starting from commercially available 1,8-dichloroanthraquinone.[9,10] The yields at each step range between 51 and 93%, which means multigram quantities of **I** are not easily accessible. Another issue with 1,8,9-trisubstituted anthracenes species is that the central ring gets dearomatised rather easily as shown by Hayes.[11] In a search for replacement of synthetically challenging 1,8,9-anthracenes, our attention turned to geminally bis(*peri*-substituted) pnictogens. These provide rather similar connectivity with respect to the central atom, which experiences two proximate *peri*-interactions. In contrast to the 1,8,9-trisubstituted anthracene manifold, the bis(*peri*-substituted) pnictogen platform provides additional angular flexibility as these molecules are not rigidly planar. Rather importantly, geminally bis(*peri*-substituted) species are synthetically much more viable. In this work we report the synthesis and characterisation of a bis(*peri*-substituted) arsine and stibine, which represent heavier homologues of ligand **H**. In addition, tris(*peri*-substituted) arsine, stibine and bismuthine are reported; these represent the first examples of a new class of rigid tetradentate (P_3E) tris(*peri*-substituted) pnictine ligands.

Results & Discussion

Syntheses

5-Bromo-6-(diisopropylphosphino)acenaphthene (**1**) was used as the principal precursor in all syntheses described in this study.[12] Low temperature lithium-halogen exchange reaction with *n*-butyllithium yielded 5-lithio-6-(diisopropylphosphino)acenaphthene (**1'**), which was, without isolation, subjected to C–E coupling with either $^1/_3$ molar equivalent of ECl_3 (E = As, Sb, Bi) or $^1/_2$ equivalent of $PhECl_2$ (E = As, Sb) (Scheme 1). After aqueous work-up under oxygen free conditions, the novel compounds **2–6** were isolated as air sensitive white to yellow powders in moderate to high yields (32–80%). All compounds **2–6** are hydrolytically stable and were fully characterised by multinuclear NMR spectroscopy (^{1}H, ^{13}C and ^{31}P), single crystal X-ray diffraction, mass spectrometry, infrared and Raman spectroscopy, with the homogeneity confirmed by microanalysis.

Dichlorophenylarsine was prepared by the SO_2 reduction of phenylarsonic acid in the presence of HCl.[13] Dichlorophenylstibine was prepared by the redistribution reaction of $SbCl_3$ and $SbPh_3$.[14,15] Multiple attempts to synthesise $PhBiCl_2$ *via* a related route resulted in the desired species being significantly contaminated by Ph_3Bi, Ph_2BiCl and $BiCl_3$ with purification by recrystallisation from various solvents proving ineffective. The subsequent reaction of this impure material with **1'** resulted in complex, inseparable mixtures.

While the bis(*peri*-substituted) tridentate phosphine **H** has been prepared by the reaction of **1'** with ½ molar equivalent of *i*PrPCl$_2$ cleanly with a good yield (68%),[8] the low temperature reaction of **1'** with 1/3 molar equivalent of PCl_3 gave a complex mixture of products (as judged by ^{31}P{^{1}H} NMR). Therefore, the tris(*peri*-substituted) phosphorus-centred congener of the series **2–4** was deemed inaccessible by this route and was not pursued further.

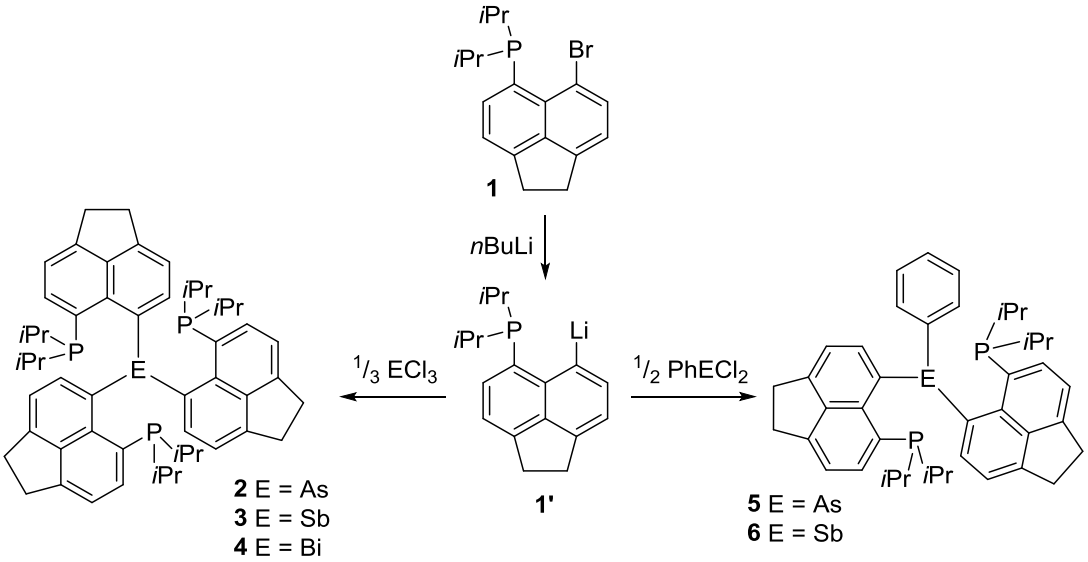

Scheme 1: Preparation of compounds **2–6**.

Structural Investigations

Tris(acenaphthene) species 2–4

Crystal structures of compounds **2–4** are shown in Figure 2, with selected data given in Table 1. In each case, the central pnictogen atom (**2** = As, **3** = Sb, **4** = Bi) adopts a trigonal pyramidal geometry, with slight increase in acuteness of the C_{ipso}–E–C_{ipso} angles following the As, Sb, Bi sequence (see Table 1). No strong dative interactions are formed between the Lewis basic *i*Pr_2P groups and the central pnictogen atom as indicated by P···E distances, which range between 3.1 and 3.3 Å. The observed positive splay angles (10.1–16.5°) further support this notion. Despite three bulky *peri*-groups being attached to the pnictogen centres in **2–4**, there are no major distortions of acenaphthene rings, with only moderate to medium in-plane and out-of-plane displacement of the *peri*-atoms observed (Table 1). More significant deviations are observed only in one of the acenaphthene rings of **3**, which shows P and Sb out-of-plane displacements of 0.60 and 0.88 Å; with the corresponding dihedral angle P19–C9···C1–Sb1 of 34.7(3)°. This is a significant increase *vs.* the other two acenaphthene moieties in this molecule; however this anomaly is readily explained through a local trade-off for decreased in-plane distortion in this particular *peri*-motif observable as a slightly diminished splay angle of 10.1°. For comparison, displacements in related singly-acenaphthene substituted *i*Pr_2P-Ace-$SbPh_2$ are 0.111 and 0.039 Å, with splay angle of 15.7(4)°.[15]

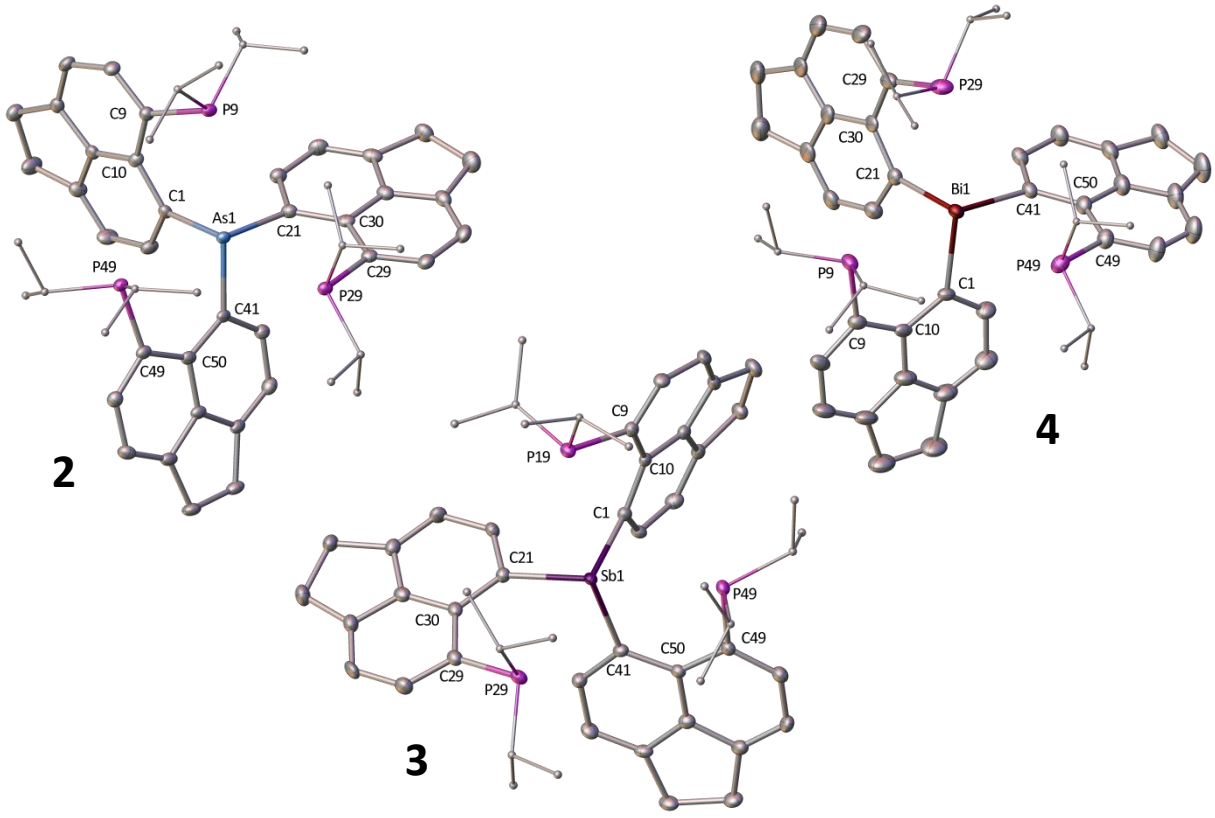

Figure 2: Crystal structures of **2**–**4**. Solvating molecules (toluene for **3** and CH_2Cl_2 for **4**) and hydrogen atoms are omitted, with isopropyl groups simplified for clarity. Ellipsoids are plotted at the 40% probability level.

Due to the specifics of the *peri*-substitution, all P···E distances are significantly sub-van der Waals (77–80% using R_{vdW} = 1.95 (P), 2.05 (As), 2.20 (Sb) and 2.30 Å (Bi)).[16] Taking these short contacts into account, the central pnictogen atom could also be viewed as attaining distorted octahedral geometry with its lone pair protruding through one of the octahedron faces. A collinear arrangement of all C_{ipso}–E···P motifs observed in the crystal structures of **2**–**4** is consistent with the onset of an n(P)→σ*(E–C) 3c–4e interaction (see Figure 9).

Due to the large size and almost spherical shape of molecules **2**–**4**, the crystals have large voids which accommodate solvent easily. In all cases (except for one incidence of **2**) minor (unmodelled) disorder of the solvent was observed in the crystal structures.

Bis(acenaphthene) species 5 and 6

The crystal structures of **5** and **6** (Figure 3, Table 1) show slight alleviation of the steric congestion around the central pnictogen atom (**5**, E = As; **6**, E = Sb) as one of the large *i*Pr_2P-Ace units has been replaced by a phenyl ring.

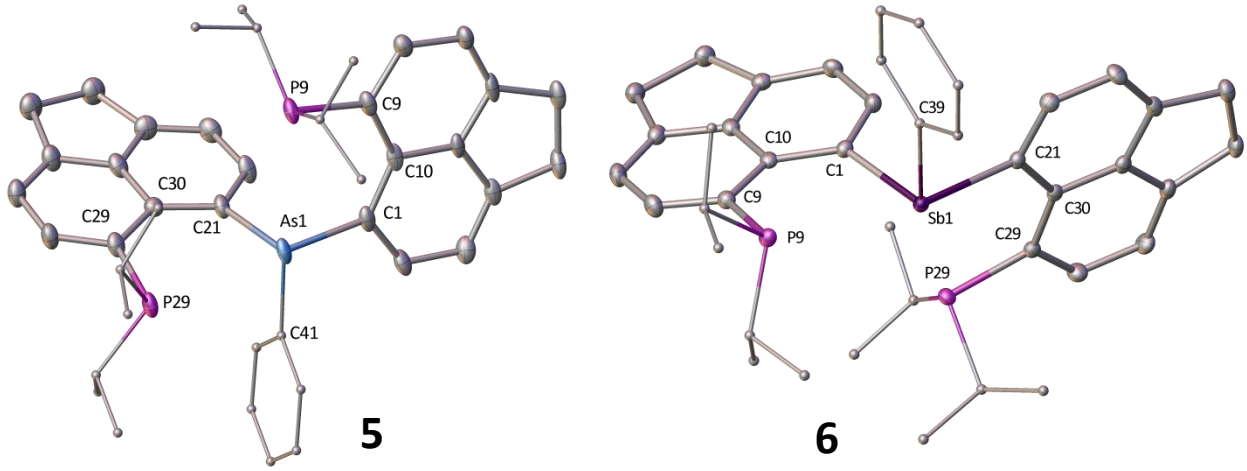

Figure 3: Crystal structures of **5** and **6.** Solvating molecules (CH_2Cl_2 for **5** and toluene for **6**) and hydrogen atoms are omitted, with isopropyl and phenyl groups simplified for clarity. Ellipsoids are plotted at the 40% probability level.

Similarly to the tris(acenaphthene) species **2**–**4**, no strong dative interactions are present between the central pnictogen atoms and the *i*Pr_2P- groups, with P···E distances in the region of 3.12–3.25 Å. The arsenic and antimony atoms attain a trigonal pyramidal geometry. Taking sub-van der Waals

contacts into account, the As and Sb atoms display distorted tetragonal pyramidal geometry formed by three carbon atoms and two proximal *i*Pr_2P- groups, with the lone pair on E atoms protruding through the base of the pyramid to complete the pseudo-octahedral coordination. There are no major distortions in either **5** or **6**, with the largest out-of-plane displacement being around 0.4 Å. The splay angles range between 14.1 and 17.1°; also the P–C···C–E dihedral angles compare well to the related parameters in compounds **2**–**4**. As above, a collinear arrangement of all C_{ipso}–E···P motifs observed in crystal structures of **5** and **6** is consistent with the onset of an n(P)→σ*(E–C) 3c–4e interaction. Similarly to the crystal structures of **2**–**4**, in both **5** and **6**, solvent was incorporated into the crystal structure due to the large voids formed on packing.

Table 1: Selected bond lengths, displacements (Å) and angles (°) for compounds **2**–**6**. Values in square brackets are for the 2nd molecule in the asymmetric unit.

	2	**3**·C_7H_8	**4**·$2CH_2Cl_2$	**5**·CH_2Cl_2	**6**·$2.5C_7H_8$
Distances					
C_{Ace}–P	1.846(3)–1.853(3)	1.832(6)–1.839(5)	1.80(2)–1.85(1)	1.837(7)–1.839(7)	1.837(2)–1.845(2)
C–E1	2.002(2)–2.021(3)	2.212(6)–2.224(5)	2.31(1)–2.34(1)	1.965(6)–2.003(7)	2.183(2)–2.214(2)
P···P	4.838(1)–5.251(1)	4.947(2)–5.484(2)	5.066(6)–5.484(5)	4.970(3)	5.2409(9)
P9···E1	3.2051(9)	3.305(1)	3.240(3) [3.279(4)]	3.120(2)	3.1684(7)
P29···E1	3.1938(8)	3.197(1)	3.250(4) [3.218(3)]	3.188(2)	3.2513(7)
P49···E1	3.162(1)	3.172(2)	3.250(3) [3.242(4)]	*n/a*	*n/a*
Angles					
C–E1–C	96.4(1)–98.7(1)	93.6(2)–97.3(2)	91.7(5)–96.0(5)	97.2(3)–100.0(3)	93.80(6)–96.04(6)
P···E1···P	98.91(2)–110.30(2)	99.59(4)–114.98(4)	103.3(1)–115.1(1)	103.97(5)	109.44(2)
Splay angles*	16.5 15.5 15.7	10.1 15.2 14.8	15.9 [16.0] 15.9 [15.7] 16.0 [16.0]	15.2 17.1	14.1 16.5
P–C···C–E1	15.5(1) 1.3(1) 8.3(1)	34.7(3) 0.0(3) 0.1(3)	2.8(7) [2.5(7)] 6.3(7) [1.5(7)] 7.4(7) [8.6(8)]	0.5(4) 9.3(4)	8.2(1) 13.3(1)
Out-of-Plane Displacements					
P	0.139–0.391	0.194–0.599	0.025–0.338	0.102–0.211	0.041–0.216
E	0.197–0.273	0.197–0.881	0.027–0.442	0.194–0.314	0.379–0.431

* Splay angle = Σ of the bay region angles – 360°.

NMR Spectroscopy

Tris(acenaphthene) species 2–4

Compounds **2**–**4** show sharp singlets at δ_P –13.0 (**2**), –19.1 (**3**) and –21.3 ppm (**4**), indicating a slight increase in shielding of the phosphorus atoms on descending group 15. Due to the crowded, propeller-like geometry of **2**–**4**, the ^{1}H and $^{13}C\{^{1}H\}$ NMR spectra display multiple anisochronous signals for chemically equivalent groups. Using **2** as an example, four CH_3 and two CH environments are observed as complex multiplets in the ^{1}H and $^{13}C\{^{1}H\}$ NMR spectra (Figure 5). The signals of methyl carbon atoms (δ_C 21.3–18.9 ppm) are second order multiplets, corresponding to AA'A''X spin systems (A = ^{31}P, X = ^{13}C). Despite considerable effort, which included acquisition of the spectra at high field (16.4 T, 700 MHz instrument) and many iterative attempts, we have not been able to simulate the spin systems to extract *J* couplings. This is because methyl carbons couple not only with ^{31}P atoms separated by two bonds ($^{2}J_{CP}$), but have also non-negligible couplings with more distant phosphorus atoms. These two couplings, with a formal separation of 10 bonds ($^{10TS}J_{CP}$), have different magnitudes, which results in a complex second order signal. The shape of the signals is very sensitive to subtle changes of the coupling constants, which made the iterative fitting impossible. Whilst we cannot determine exact magnitude of these long range couplings, we can confirm both these $^{10TS}J_{CP}$ couplings are very likely non-negligible (i.e. > 2 Hz) and different in each of the four diastereotopic methyl groups in **2**–**4**. The through–bond component (through ten bonds, ^{10}J), is likely to be very small, if not zero.[17] Hence, it is highly likely that the couplings involve two through space components (through two *peri*-gaps), i.e. the magnetisation is transferred due to the overlap of lone pairs on each of the two phosphorus atoms with the lone pair on the central arsenic atom (Figure 4).

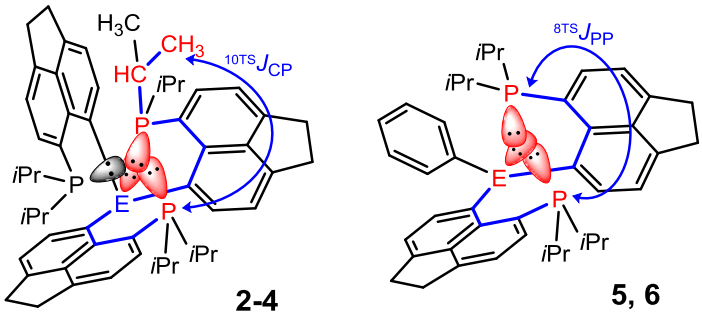

Figure 4: Graphical representation of the magnetisation transfer pathway in long range couplings. Bonds (formally) involved in the transfer are shown in blue and lone pairs involved in the transfer (through space) are shown in red. Left: One of the $^{10TS}J_{CP}$ couplings between a CH_3 carbon atom and a distant P atom in molecules **2**-**4**. Right: $^{8TS}J_{PP}$ coupling between the two P atoms in molecules **5** and **6**.

In a similar vein, isopropyl CH environments (δ_C 26.8–25.8 ppm in **2**) display complex multiplets, corresponding to AA'A''X spin systems (Figure 5).

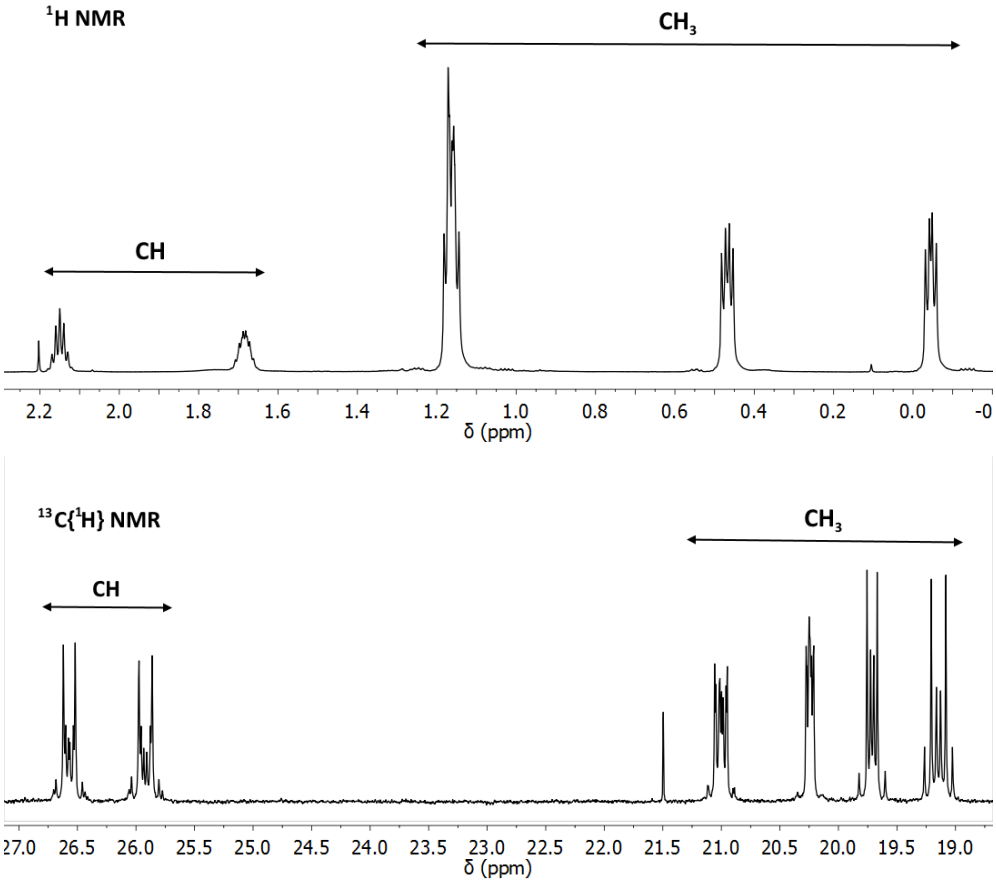

Figure 5: NMR spectra of **2**, the alkyl region of the ^{1}H NMR spectrum (recorded at 700.1 MHz) (top) and the alkyl region of the ^{13}C{^{1}H} NMR spectrum (recorded at 176.1 MHz) (bottom).

Low temperature (222 K) ^{31}P{^{1}H} NMR spectra of **2**–**4** did not display any observable line broadening or other notable changes, indicating no additional interlocking takes place at this temperature.

Bis(acenaphthene) species 5 and 6

The ^{31}P{^{1}H} NMR spectrum of **5** in d_8-toluene (121.5 MHz, 298 K) shows two broad resonances at δ_P –11.5 and –14.4 ppm (Figure 6). This is consistent with the molecule experiencing restricted rotational dynamics in the solution, presumably around the As–C_{Acenap} bonds (As1–C1 and As1–C21, see Figure 3). In line with this, all signals in the ^{1}H NMR spectrum of **5** (298 K, 300.1 MHz) were broadened, whilst very broad signals were observed in the ^{13}C{^{1}H} NMR spectrum at the same temperature (75.5 MHz) (see supporting info).

In order to gain insight into the dynamic behaviour of **5**, a variable temperature NMR study was performed in a range of 223–373 K (Figure 6). Upon warming the sample of **5** to 373 K, a singlet was observed in the ^{31}P{^{1}H} NMR spectrum at δ_P –10.5 ppm, indicating that the two phosphorus environments interchange rapidly at this temperature. Upon cooling to 223 K, the ^{31}P{^{1}H} NMR

spectrum revealed two sharp doublets at δ_P –13.2 and –16.9 ($^{8TS}J_{PP}$ 11.5 Hz), consistent with a simple AX spin system. The magnitude of $^{8TS}J_{PP}$ is remarkable since there is no direct overlap of the lone pairs on phosphorus atoms. The transfer of magnetisation is highly likely to involve two through space interactions due to the overlap of the two phosphorus lone pairs with the diffuse arsenic lone pair (n(P)···n(As) ···n(P) interaction, Figure 4).

Detailed lineshape analysis of the $^{31}P\{^1H\}$ VT NMR spectra (see Figure S18 in supporting information for Eyring plot) yielded thermodynamic parameters of $\Delta H^{\neq}$ = 57.1 kJ mol^{-1} and $\Delta S^{\neq}$ = –17.5 J mol^{-1} K^{-1} for the interchange process in **5**. For completeness, the coalescence method gave a rotational barrier $\Delta G^{\neq}$ of 62.3 kJ mol^{-1} at 340 K for **5**. These data complement those obtained on the related tris(phosphine) **H**, mentioned above. Due to the complexity of the dynamic processes in tris(phosphine) **H**, in which two ABC spin systems were present in the slow motion regime, the interchange process (equivalent to that described for **5**) was masked, hence precluding determination of the exchange barrier through either lineshape analysis or the coalescence method.

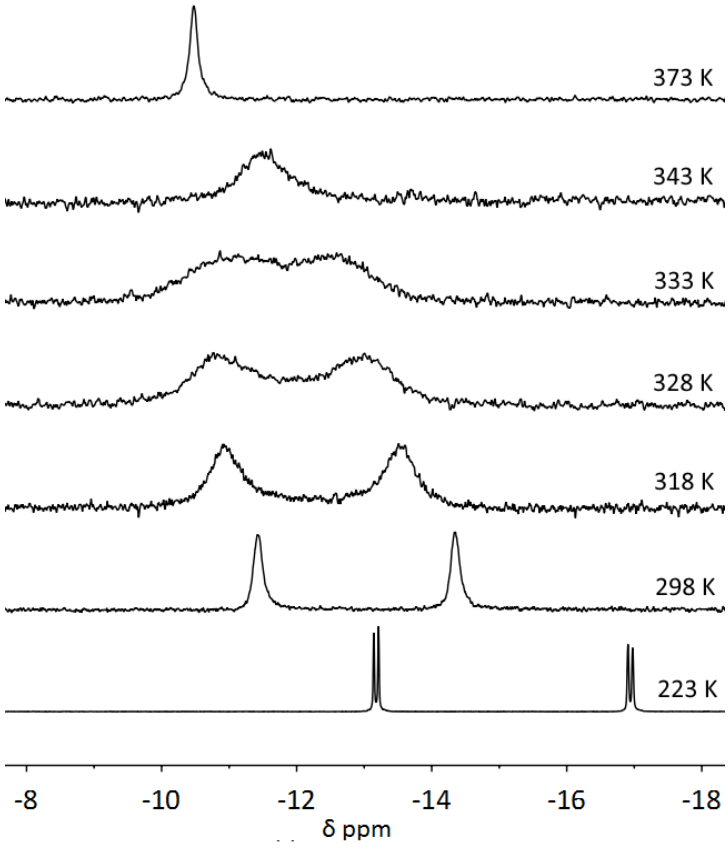

Figure 6: Variable temperature $^{31}P\{^1H\}$ NMR spectra of **5** in d_8-toluene at 121.5 MHz.

Compound **6** shows similar features to its arsenic homologue **5**. The $^{31}P\{^1H\}$ NMR spectrum of **6** at 298 K (109.4 MHz) shows an extremely broad resonance (Figure 7). A variable temperature NMR study revealed a sharp singlet (δ_P –17.5 ppm) at 363 K (fast motion regime), and two sharp

doublets (δ_P –21.2 and –24.2 ppm) at 223K (slow motion regime). The increased magnitude of $^{8TS}J_{PP}$ between **5** and **6** (11.5 Hz *vs.* 25.8 Hz, both at 223 K) can be attributed to the larger antimony atom acting as a more efficient mediator of magnetic spin information between the two phosphorus atoms (see Figure 4). The coalescence temperature of **6** was 303 K (at 109.4 MHz), which corresponds to the rotational barrier $\Delta G^{\neq}$ of 62.0 kJ mol^{-1}. This is remarkably similar to the energy barrier associated with interchange in **5**, obtained from the detailed lineshape analysis ($\Delta G^{\neq}$ = 62.4 kJ mol^{-1} at 303 K).

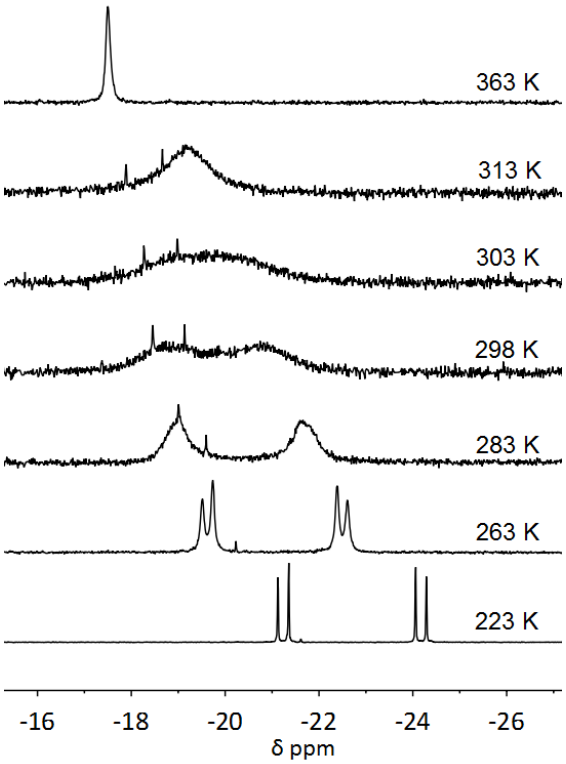

Figure 7: Variable-temperature $^{31}P\{^1H\}$ NMR spectra of **6** in d_8-toluene at 109.4 MHz. Minor peaks are from unrelated impurity.

Computational Investigations

To complement these findings, we performed calculations at the B3LYP-D3/6-31G* level of density functional theory (DFT). Taking the arsenic compounds **2** and **5** as representatives, their structures were optimised starting from the single crystal X-ray coordinates, and their wavefunctions were subjected to natural bond orbital (NBO) analysis.[18] The distances between the formally non-bonded As and P atoms are reasonably well reproduced at that level, e.g. for the mean As···P distance in **2** (DFT: 3.151 Å, X-ray: 3.189 Å).[19] The localised lone pairs on phosphorus and arsenic atoms are visualised in Figure 8; these are somewhat "buried" within the molecules, in particular for the

tris(acenapthene) derivative **2**, indicating they may not be readily available for coordination chemistry.

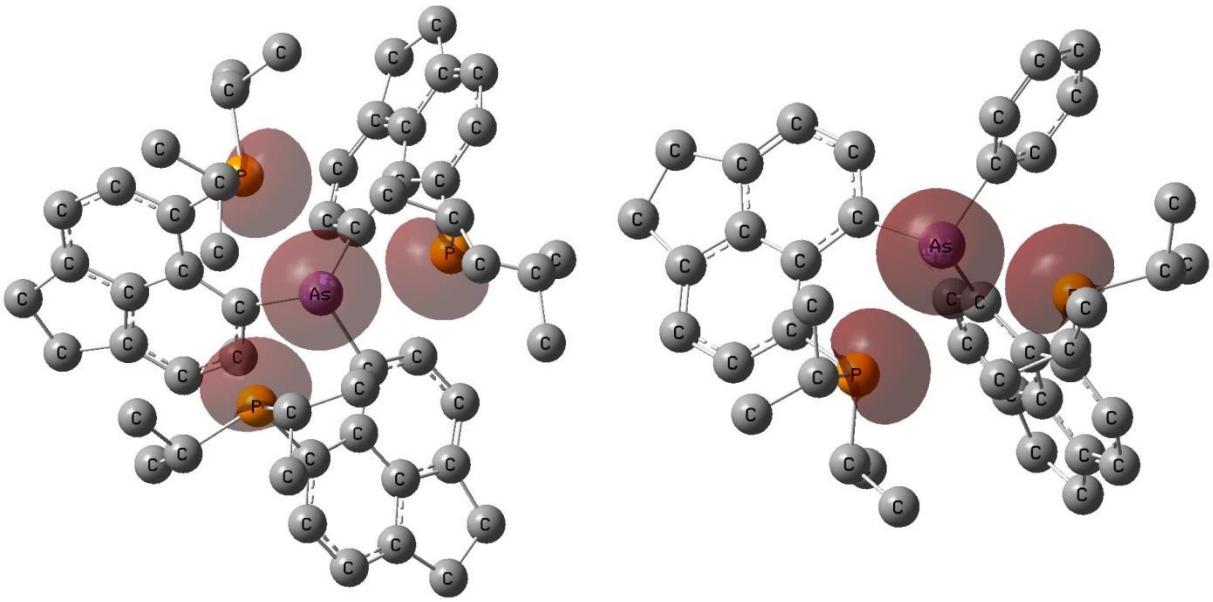

Figure 8: Plot of the lone pair NBOs in compounds **2** (left) and **5** (right). Hydrogen atoms are omitted for clarity, isodensity values are 0.08 au. Molecules are viewed from "above" looking down the As lone pair; for other views see SI.

Arguably, there is repulsion between the lone pairs on As and P atoms. There are, however, weak attractions between these atoms counteracting this repulsion. In a second-order perturbation analysis these are identified as n(P)→σ*(As-C_{ipso}) dative interactions worth *ca.* 10 to 11 kcal/mol each (for one of them, the relevant pair of NBOs is depicted in Figure 9). These interactions are likely to support the collinear arrangement of C_{ipso}–E···P motifs observed throughout the crystal structures of **2**–**5**. These dative interactions give rise to notable Wiberg bond indices (WBIs) between the arsenic and phosphorus atoms, on the order of 0.10 to 0.11.[20] Slightly lower, but still notable WBIs (ca. 0.07 to 0.09) and donor–acceptor energies (ca. 7–9 kcal/mol) are obtained at the same DFT level when the X-ray structures are employed without minimisation. Similar characteristics have been found between other heavier chalcogen and pnictogen atoms in *peri*-naphthalene positions, where such notable dative interactions and WBIs have been taken as evidence for the onset of multicentre bonding.[15,21,22]

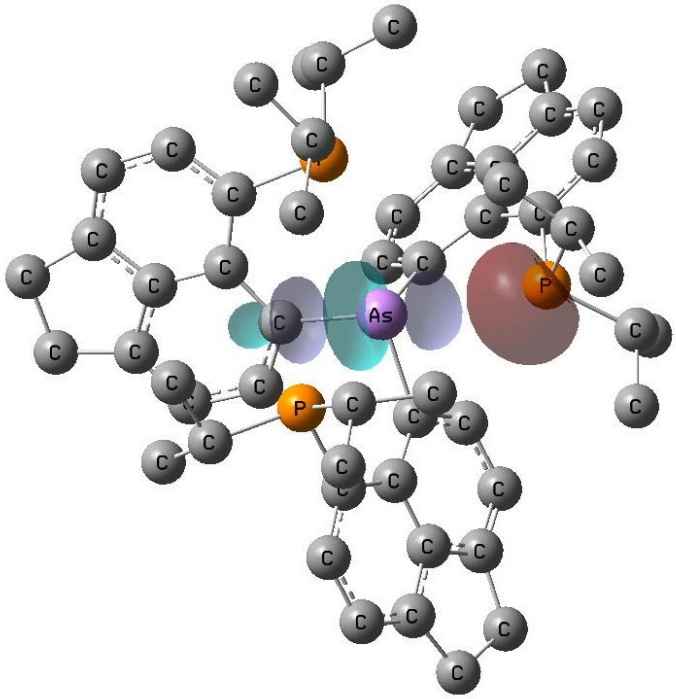

Figure 9: Plot of one pair of NBOs involved in dative interactions in **2**; red: lone pair donor on P, grey/turquoise: antibonding σ*(As–C) acceptor orbital. H atoms are omitted for clarity, isodensity values are 0.08 au.

Conclusion

Detailed structural and NMR spectroscopic study of bis(phosphinoacenaphthene) and tris(phosphinoacenaphthene) pnictines confirmed the sterically crowded nature of these molecules, with sub-van der Waals P···E contacts across the *peri*-region. However, relatively high yields and moderate acenaphthene ring distortions indicate that the blade-like arrangement of the substituents in these propeller-shaped molecules is rather accommodating. The relative simplicity of the $^{31}P\{^{1}H\}$ NMR spectra of **5** and **6** at low temperatures allowed determination of the long range $^{8TS}J_{PP}$ couplings. Their magnitudes (11.5 and 25.8 Hz) are remarkable. The transfer of magnetisation is likely to involve two through-space interactions in which the central pnictogen's lone pair acts as a "relay", i.e. n(P)···n(E)···n(P) interactions (E = As, Sb) take place. This is because the direct overlap of the two phosphorus atoms is ineffective, the P···P distances ranging from 4.838(1) to 5.484(5) Å (see Table 1 and the plot of the lone pair NBOs in Figure 8). The lone pairs on the pnictogen atoms form a bowl-like environment, which however, is somehow buried within the molecule. Coordination chemistry of these potential tetradentate (**2**-**4**) and tridentate (**5**, **6**) ligands will be studied next.

Experimental

General Considerations

All reactions and manipulations were carried out under an atmosphere of nitrogen using standard Schlenk techniques or under an argon atmosphere in a Saffron glove box. Dry solvents were either collected from an MBraun Solvent Purification System, or dried and stored according to common procedures.[23] Compound **1** was prepared according to the published procedure.[12] Antimony trichloride was purchased from Sigma-Aldrich and purified by vacuum sublimation before use. Dichlorophenylarsine ($PhAsCl_2$)[13] and dichlorophenylstibine ($PhSbCl_2$)[14,15] were prepared according to the published procedures; further details are in the supporting information. Other chemicals were purchased from Acros Organics, Sigma Aldrich or Alfa Aesar and used as received. *Caution! Organoarsenic halides and arsenic halides are powerful vessicants, which cause severe irritation and blistering if allowed to come in contact with skin.* Suitable precautions, including the use of neoprene or rubber gloves when handling these, should be taken. Further experimental details are provided in SI.

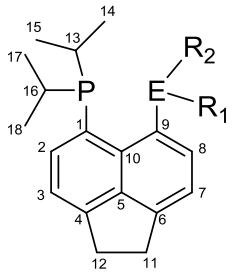

E = As, Sb, Bi
R_1 = *i*Pr_2P-Ace
R_2 = *i*Pr_2P-Ace, Ph

Figure 10: NMR numbering scheme for compounds **2**–**6**.

Synthetic Methods

(*i*Pr_2P-Ace)$_3$As (2):

To a cooled (–78 °C) stirred solution of **1** (3.75 g, 10.7 mmol) in diethyl ether (100 mL), *n*-butyllithium (4.30 mL, 2.5 M in hexanes, 10.7 mmol) was added dropwise over one hour. The resulting solution was left to stir for a further one hour at –78 °C. To this, a solution of arsenic trichloride (300 µL, 65 mg, 3.6 mmol) in diethyl ether (10 mL) was added dropwise over two hours. The solution was left to warm to ambient temperature overnight. The volatiles were removed *in vacuo* and replaced with toluene (100 mL). The solution was washed with degassed water (45 mL) and the organic layer dried over magnesium sulfate. After filtration, the volatiles were again removed *in vacuo* to give a yellow

powder (7.58 g, 80%) (M.p. >250 °C). Crystals suitable for X-ray diffraction work were grown from chloroform at room temperature. **^{1}H NMR:** δ_H (700.1 MHz, $CDCl_3$) 7.62 (3H, dd, $^{3}J_{HH}$ = 7.1, $^{7ts}J_{HP}$ = 1.7 Hz, H-8), 7.57 (3H, d, $^{3}J_{HH}$ = 7.1 Hz, H-2), 7.29 (3H, m, H-7), 6.86 (3H, d, $^{3}J_{HH}$ = 7.1 Hz, H-3), 3.43–3.24 (12H, m, H-11,12), 2.15 (3H, h, $^{3}J_{HH}$ = 6.8 Hz, H-16), 1.72–1.65 (3H, m, H-13), 1.19–1.13 (18H, m, H-17,18), 0.47 (9H, dd, $^{3}J_{HP}$ = 13.4, $^{3}J_{HH}$ = 6.7 Hz, H-15), –0.04 (9H, dd, $^{3}J_{HP}$ = 12.1, $^{3}J_{HH}$ = 7.0 Hz, H-14). **^{13}C{^{1}H} NMR:** δ_C (176.1 MHz, $CDCl_3$) 147.9 (s, qC-6), 145.7 (s, qC-4), 143.1–142.5 (m, $^{1}J_{CP}$ ≈ 49 Hz, qC-1), 141.0–140.7 (m, ~dt, $^{2}J_{CP}$ ≈ 29Hz, qC-10), 140.5 (s, C-2), 140.2–140.1 (m, qC-5), 133.8 (s, C-8), 132.4–132.0 (m, , qC-9), 119.6 (s, C-3), 118.2 (s, C-7), 30.1 (s, C-11/12), 29.6 (s, C-11/12), 26.8–26.4 (m, C-16), 26.1–25.8 (m, C-13), 21.1–20.9 (m, C-18), 20.3–20.1 (m, C-17), 19.8–19.6 (m, C-14), 19.2–18.9 (m, C-15). **^{31}P{^{1}H} NMR:** δ_P (202.5 MHz, $CDCl_3$) –13.0 (s). **Infrared data** (KBr disc, cm^{-1}) ν = 3021w ($\nu_{Ar–H}$), 2921vs ($\nu_{C–H}$), 1871m, 1607s, 1319s, 842vs. **Raman data** (glass capillary, cm^{-1}) ν = 3061m ($\nu_{Ar–H}$), 2929s ($\nu_{C–H}$), 1607s, 1561s, 1466s, 1412s, 1322vs, 580s. **Elemental Analysis** Calculated for $C_{54}H_{66}P_3As$: C 73.46, H 7.53. Found: C 73.28, H 7.45. **HRMS (APCI+):** *m/z* (%): Calcd. for $C_{54}H_{67}P_3As$: 883.3666, found 883.3647 (100) [M+H$^+$]; Calcd. for $C_{36}H_{44}P_2As$: 613.2134, found 613.2109 (45) [M–*i*Pr_2P-Ace]; Calcd. for $C_{18}H_{23}PAs$: 345.0753, found 345.0738 (5) [M– 2 × *i*Pr_2P-Ace + H].

(*i*Pr_2P-Ace)$_3$Sb (3):

Compound **3** was prepared using the same procedure as per compound **2** except using the following quantities: **1** (3.00 g, 8.6 mmol) in diethyl ether (100 mL); *n*-butyllithium (3.4 mL, 2.5 M in hexanes, 8.6 mmol); antimony trichloride (650 mg, 2.9 mmol) in diethyl ether (8 mL); toluene (50 mL); degassed water (25 mL) giving a yellow powder (2.46 g, 32%) (Mp. >250 °C). Crystals suitable for X-ray diffraction work were grown from toluene at –35 °C. **^{1}H NMR:** δ_H (500.1 MHz, $CDCl_3$) 7.85 (3H, d, $^{3}J_{HH}$ = 6.6 Hz, H-2), 7.61 (3H, d, $^{3}J_{HH}$ = 6.2 Hz, H-8), 7.29 (3H, d, $^{3}J_{HH}$ = 7.3 Hz, H-7), 6.84 (3H, d, $^{3}J_{HH}$ = 6.9 Hz, H-3), 3.40-3.25 (12H, m, H-11, 12), 2.14 (3H, h, $^{3}J_{HH}$ = 6.8 Hz, H-16), 1.88 (3H, dh, $^{2}J_{HP}$ = 13.5, $^{3}J_{HH}$ = 6.8 Hz, H-13), 1.21 (9H, m, H-18), 1.16 (9H, m, H-17), 0.56 (9H, m, H-14), 0.11 (9H, m, H-15). **^{13}C{^{1}H} NMR:** δ_C (125.8 MHz, $CDCl_3$) 148.3 (s, qC-6), 145.7 (d, $^{1}J_{CP}$ = 57.6 Hz, qC-1), 145.2 (s, qC-4), 143.2 (s, C-2), 143.0–142.8 (m, qC-10), 140.0–139.8 (m, qC-5), 133.2 (s, C-8), 131.8–131.5 (m, qC-9), 120.2 (s, C-3), 118.2 (s, C-7), 30.2 (s, C-11/12), 29.9 (s, C-11/12), 27.1–26.8 (m, C-16), 25.6–25.4 (m, C-13), 21.0–20.8 (m, C-18), 20.0–19.9 (m, C-17), 19.8–19.7 (m, C-15), 19.6–19.5 (m, C-14). **^{31}P NMR:** δ_P (202.5 MHz, $CDCl_3$) −19.1 (s). **Infrared data** (KBr disc, cm^{-1}) ν = 3024w ($\nu_{Ar–H}$), 2922vs, 2864vs ($\nu_{C–H}$), 1604s, 1587s, 1461s, 1320s. **Raman data** (glass capillary, cm^{-1}) ν = 3059m ($\nu_{Ar–H}$), 2926vs ($\nu_{C–H}$), 2870s ($\nu_{C–H}$), 1321vs, 579s. **Elemental Analysis:** Calculated for $C_{54}H_{66}P_3Sb$: C 69.76, H 7.15. Found: C 69.63, H 7.27. **HRMS (APCI+):** *m/z* (%): Calcd. for $C_{54}H_{67}P_3Sb$: 929.3488, found 929.3496 (12) [M+H$^+$]; Calcd. for $C_{36}H_{44}P_2Sb$: 659.1951, found 659.1956 (100) [M-*i*Pr_2P-Ace].

(iPr_2P-Ace)$_3$Bi (4):

To a cooled (–78 °C) rapidly stirring stirred solution of **1** (1.00 g, 2.86 mmol) in diethyl ether (25 mL), *n*-butyllithium (1.2 mL, 2.5 M in hexanes, 2.95 mmol) was added dropwise over 30 minutes. The resulting yellow suspension was stirred for 3 hours at this temperature. A cooled (–78 °C) suspension of $BiCl_3$ (296 mg, 0.94 mmol) in diethyl ether (30 mL) was prepared and stirred rapidly. The first suspension was added *via* cannula to the $BiCl_3$ with the mixture stirred for 1.5 hours at this temperature. The reaction was allowed to warm to ambient temperature overnight resulting in a white precipitate which was collected *via* filtration. The solid was washed with diethyl ether (2 × 10 mL) then degassed water (10 mL) and dried *in vacuo* for 4 hours. The product was obtained as a white powder (300 mg, 0.29 mmol, 32%). (Mp. 202–203 °C decomp.). X-ray quality crystals of **4** were grown from a saturated solution in dichloromethane at 0 °C. **^{1}H NMR:** δ_H (500.1 MHz, $CDCl_3$) 8.60 (3H, dd, $^3J_{HH}$ = 6.9, $^{7ts}J_{HP}$ = 2.4 Hz, H-8), 7.60 (3H, dd, $^3J_{HH}$ = 7.2, $^3J_{HP}$ = 2.8 Hz, H-2), 7.27 (3H, d, $^3J_{HH}$ = 7.1 Hz, H-3), 6.85 (3H, d, $^3J_{HH}$ = 6.8 Hz, H-7), 3.38–3.19 (12H, m, H11/12), 2.10 (3H, h, $^3J_{HH}$ = 6.9 Hz, H-16), 1.89 (3H, h, $^3J_{HH}$ = 6.8 Hz, H-13), 1.22 (9H, dd, ~q, $^3J_{HP}$ = 13.4, $^3J_{HH}$ = 7.0 Hz, H-17), 1.12 (9H, dd, ~q, $^3J_{HP}$ = 10.1, $^3J_{HH}$ = 6.9 Hz, H-18), 0.63 (9H, dd, ~q, $^3J_{HP}$ = 14.4, $^3J_{HH}$ = 6.8 Hz, H-14), 0.17 (9H, dd, ~q, $^3J_{HP}$ = 12.6, $^3J_{HH}$ = 6.9 Hz, H-15). **^{13}C NMR:** δ_C (125.8 MHz, $CDCl_3$) 176.6 (s, qC-9), 148.8 (s, qC-4), 146.6 (s, C-8), 145.3–144.9 (m, qC-10), 144.0 (s, qC-6), 141.5–141.3 (m, qC-5), 132.7 (s, C-2), 132.6–132.4 (m, qC-1), 123.5 (s, C-7), 117.9 (s, C-3), 130.2 (s, C-11/12), 130.1 (s, C-11/12), 27.0–26.7 (m, C-16), 25.5–25.3 (m, C-13), 21.5–21.2 (m, C-18), 20.3–20.1 (m, C-17), 19.9–19.5 (m, C14,15). **^{31}P{^{1}H} NMR:** δ_P (202.5 MHz, $CDCl_3$) –21.3 (s). **Infrared data:** (KBr disc, cm^{-1}): ν = 3022w ($\nu_{Ar–H}$), 2948s ($\nu_{C–H}$), 1631br, 1460s, 1322s, 1245s. **Raman data:** (glass capillary, cm^{-1}): ν = 3048m ($\nu_{Ar–H}$), 1570m, 999s, 211s. **Elemental Analysis** Calculated for $C_{54}H_{66}P_3Bi$: C 63.77, H 6.46. Found: C 63.64, H 6.46. **HRMS** (APCI+): *m/z* (%); Calcd. for $C_{54}H_{67}P_3Bi$: 1017.4244, found 1017.4254 [M+H$^+$].

(iPr_2P-Ace)$_2$AsPh (5):

To a cooled (–78 °C), rapidly stirring solution of **1** (3.00 g, 8.6 mmol) in diethyl ether (75 mL) *n*-butyllithium (3.5 mL, 2.5 M solution in hexanes, 8.6 mmol) was added over a period of one hour and the mixture was left to stir for two hours at the same temperature. A solution of dichlorophenylarsine (0.96 g, 0.58 mL, 4.6 mmol) in diethyl ether (10 mL) was added dropwise over one hour and the resulting solution left to warm to ambient temperature overnight. Additional diethyl ether (110 mL) was added, along with degassed water (25 mL), and the solution was stirred vigorously for 10 minutes. The organic layer was separated and dried over magnesium sulfate. The volatiles were removed *in vacuo* to give a yellow powder that was dried *in vacuo* for 3 hours (1.91 g,

64%) (Mp. 160 °C). X-ray quality crystals of **5** were grown from dichloromethane at –35 °C. **^{1}H NMR:** δ_H (300.1 MHz, d_8-toluene, 298 K) 7.76 (br s,), 7.56 (br s), 7.59 (br s), 6.93 (br s), 6.75 (br s), 2.97 (br s, H-11,12), 2.47 (br s), 2.16 (br s), 1.98 (br s), 1.85 (br s), 1.51 (3H, br s, 1 × CH_3), 1.46 (3H, br s, 1 × CH_3), 1.29 (3H, br s, 1 × CH_3), 1.09 (3H, br s, 1 × CH_3), 1.03 (3H, br s, 1 × CH_3), 0.57 (3H, br s, 1 × CH_3), 0.33 (3H, br s, 1 × CH_3), 0.15 (3H, br s, 1 × CH_3). **^{1}H NMR:** δ_H (300.1 MHz, d_8-toluene, 223 K) 8.19 (1H, d, $^{3}J_{HH}$ = 7.2 Hz, H-8), 7.90 (1H, dd, $^{3}J_{HH}$ = 7.2, $^{3}J_{HP}$ = 2.2 Hz, H-2), 7.66 (1H, d, $^{3}J_{HH}$ = 7.1 Hz, H-8'), 7.61 (1H, dd, $^{3}J_{HH}$ = 7.2, $^{3}J_{HP}$ = 3.1 Hz, H-2'), 7.54 (1H, dd, $^{3}J_{HH}$ = 7.3 Hz, $^{3}J_{HP}$ = 3.0 Hz, H-21), 7.51 (1H, d, $^{3}J_{HH}$ = 7.5 Hz, H-20), 7.40 (1H, *pseudo* dd $^{3}J_{HH}$ = 7.5 Hz, H-22), 7.22–7.15 (2H, m, H-20',21'), 7.05–6.99 (2H, m, H-3',7'), 6.96 (1H, d, $^{3}J_{HH}$ = 7.2 Hz, H-3), 6.79 (1H, d, $^{3}J_{HH}$ = 7.2 Hz, H-7), 3.08–2.85 (8H, m, H-11,11',12,12'), 2.51 (1H, h, $^{3}J_{HH}$ = 7.0 Hz, H-13), 1.95 (1H, h, $^{3}J_{HH}$ = 6.8 Hz, H-13'), 2.16 (1H, br s, H-16), 1.84 (1H, h, $^{3}J_{HH}$ = 6.7 Hz, H-16'), 1.56 (3H, dd, $^{3}J_{HP}$ = 12.6, $^{3}J_{HH}$ = 7.2 Hz, 1 × CH_3), 1.50 (3H, dd, $^{3}J_{HP}$ = 11.5, $^{3}J_{HH}$ = 6.9 Hz, 1 × CH_3), 1.13–1.04 (6H, m, 2 × CH_3), 0.61 (3H, dd, $^{3}J_{HP}$ = 15.7, $^{3}J_{HH}$ = 6.6 Hz, 1 × CH_3), 0.35 (3H, dd, $^{3}J_{HP}$ = 13.2 $^{3}J_{HH}$ = 6.8 Hz, 1 × CH_3), 0.22 (3H, $^{3}J_{HP}$ = 13.5, $^{3}J_{HH}$ = 6.7 Hz, 1 × CH_3).**^{13}C{^{1}H} NMR:** (75.5 MHz, d_8-toluene, 298 K) no signals were observed due to extreme broadening. **^{13}C{^{1}H} NMR:** (75.5 MHz, d_8-toluene, 223 K) low solubility prevented acquisition of the spectrum. **^{31}P{^{1}H} NMR:** δ_P (162.0 MHz, d_8-toluene, 293 K) –11.6 (s), –14.4 (s). **^{31}P{^{1}H} NMR:** δ_P (162.0 MHz, d_8-toluene, 223 K) –13.2 (d, $^{8ts}J_{PP}$ = 11.5 Hz) , –16.9 (d, $^{8ts}J_{PP}$ = 11.5 Hz). **^{31}P{^{1}H} NMR:** δ_P (162.0 MHz, d_8-toluene, 373 K) –10.5 (s). **Infrared data** (KBr disc, cm^{-1}) ν = 3064w (ν_{Ar-H}), 2947vs (ν_{C-H}), 1872m, 1460s, 1319s, 840s, 736s. **Raman data** (glass capillary, cm^{-1}) ν = 3066m (ν_{Ar-H}), 2948s (ν_{C-H}), 1607s, 1564s, 1445s, 1322vs, 582s. **Elemental Analysis:** Calcd. (%) for $C_{42}H_{49}P_2As{\cdot}½CH_2Cl_2$: C 69.62, H 6.87. Found: C 69.61, H 6.62. **HRMS** (APCI+): *m/z* (%): Calcd. for $C_{42}H_{50}P_2As$: 691.2598, found 691.2604 (10) [M+H$^+$]; Calcd. for $C_{36}H_{44}P_2As$: 613.2129, found 613.2127 (55) [M–Ph]; Calcd. for $C_{18}H_{22}PAs$: 421.1066, found 421.1060 (100) [M–*i*Pr_2P-Ace].

(*i*Pr_2P-Ace)$_2$SbPh (6):

Compound **6** was prepared using the same procedure as per compound **5** except using the following quantities: **1** (1.00 g, 2.90 mmol) in diethyl ether (30 mL); *n*-butyllithium (1.1 mL, 2.5 M in hexanes, 2.90 mmol); dichlorophenylstibine (390 mg, 1.45 mmol) in diethyl ether (20 mL); additional diethyl ether (25 mL); degassed water (10 mL) giving a yellow powder (1.63 g, 77%) (Mp. 165–167 °C). Crystals suitable for X-ray diffraction work were grown from toluene at ambient conditions.

^{1}H NMR: δ_H (500.1 MHz, d_8-toluene, 298 K) 8.02 (1H, d, $^{3}J_{HH}$ = 7.0 Hz,), 7.86–7.78 (m), 7.56 (dd, $^{3}J_{HH}$ = 7.1, $^{3}J_{HP}$ = 3.5 Hz), 7.20–7.06 (m), 6.75 (br s), 7.02 (br s), 6.99 (br s), 6.83 (br s), 2.99 (br s, H-11,12), 2.13–2.06 (m), 2.16 (br s), 2.08–1.88 (m), 1.59–0.08 (12H, v. br s, 8 × CH_3). **^{1}H NMR:** δ_H (400.1 MHz, d_8-toluene, 223 K) 8.16 (br s), 7.56 (br s), 7.47 (br s), 7.28–6.87 (br m), 3.06–2.77 (br s, H-11,12),

2.24–2.07 (br s, H-13), 2.00–1.82 (br s, H-13), 1.47 (3H, dd, $^{3}J_{HP}$ = 14.7, $^{3}J_{HH}$ = 7.1 Hz, 1 × CH_3), 1.37–0.99 (6H, m, 2 × CH_3), 0.73 (3H, dd, $^{3}J_{HP}$ = 15.6, $^{3}J_{HH}$ = 6.9 Hz, 1 × CH_3), 0.53 (3H, dd, $^{3}J_{HP}$ = 14.0, $^{3}J_{HH}$ = 6.9 Hz, 1 × CH_3), 0.20 (3H, dd, $^{3}J_{HP}$ = 14.1, $^{3}J_{HH}$ = 7.1 Hz, 1 × CH_3). **$^{13}C\{^{1}H\}$ NMR:** (75.5 MHz, d_8-toluene, 298 K) no signals were observed due to extreme broadening. **$^{13}C\{^{1}H\}$ NMR:** (75.5 MHz, d_8-toluene, 223 K) low solubility prevented acquisition of the spectrum. **$^{31}P\{^{1}H\}$ NMR:** δ_P (162.0 MHz, d_8-toluene, 298 K) –17.2 – –22.2 (v. br s). **$^{31}P\{^{1}H\}$ NMR:** δ_P (109.4 MHz, d_8-toluene, 363 K) – 17.5 (s). **$^{31}P\{^{1}H\}$ NMR:** δ_P (109.4 MHz, d_8-toluene, 223 K) −21.2 (d, $^{8ts}J_{PP}$ = 25.8 Hz), −24.2 (d, $^{8ts}J_{PP}$ = 25.8 Hz). **Infrared data** (KBr disc, cm^{-1}) ν = 3057m (ν_{Ar-H}), 2922vs (ν_{C-H}), 2824vs (ν_{C-H}), 1601s, 1461s, 1247s, 844s. **Raman data** (glass capillary, cm^{-1}) ν = 3049m (ν_{Ar-H}), 2928m (ν_{C-H}), 2858m (ν_{C-H}), 1603m, 1328 vs. **Elemental Analysis** Calcd. (%) for $C_{42}H_{49}P_2Sb$: C 68.40, H 6.70; Found: C 68.35, H 6.76. **HRMS** (APCI+): *m/z* (%); Calcd. for $C_{42}H_{50}P_2Sb$: 737.2420, found 737.2415 (65) [M+H^+], Calcd. for $C_{36}H_{44}P_2Sb$: 659.1956, found 659.1945 (100) [M–Ph].

X-ray Diffraction

The crystallographic details relating to this work can be found in the Supporting Information. CCDC 1476664-1476668 contain the crystallographic data for this paper. These data can be obtained free of charge from The Cambridge Crystallographic Data Centre via www. ccdc.cam.ac.uk/data_request/cif. Multiple data collections of all samples (**2**–**6**) were obtained, with crystals grown from a variety of solvents. The best quality datasets were used for refinements. In all but one case (**2**) solvent was incorporated into the crystals. Due to the close-spherical shape of molecules **2**–**6**, the incorporation of disordered solvent into the crystals could not be prevented. Although some of the crystal data sets appear of lower quality upon first inspection, they are sufficient to demonstrate the connectivity for the purposes of this work.

Acknowledgements

This work was financially supported by the EPSRC and COST actions CM0802 PhoSciNet and SM1302 SIPs. The authors would like to thank the University of St Andrews NMR Service and the EPSRC UK National Mass Spectrometry Facility at Swansea University (NMSF).

Author Information

Corresponding author

Email: pk7@st-andrews.ac.uk

Notes

The author declares no competing financial interest.

Supporting Information

The Supporting Information is available free of charge on the ACS Publications website at DOI: XXX

Further synthetic details, NMR spectra of compounds **2**–**6**, $^{31}P\{^{1}H\}$ VT NMR of **5** and **6** (including Eyring plot for **5**), further X-ray diffraction details, additional computational details and coordinates of the DFT-optimised structures.

Table of Contents Graphic and Synopsis

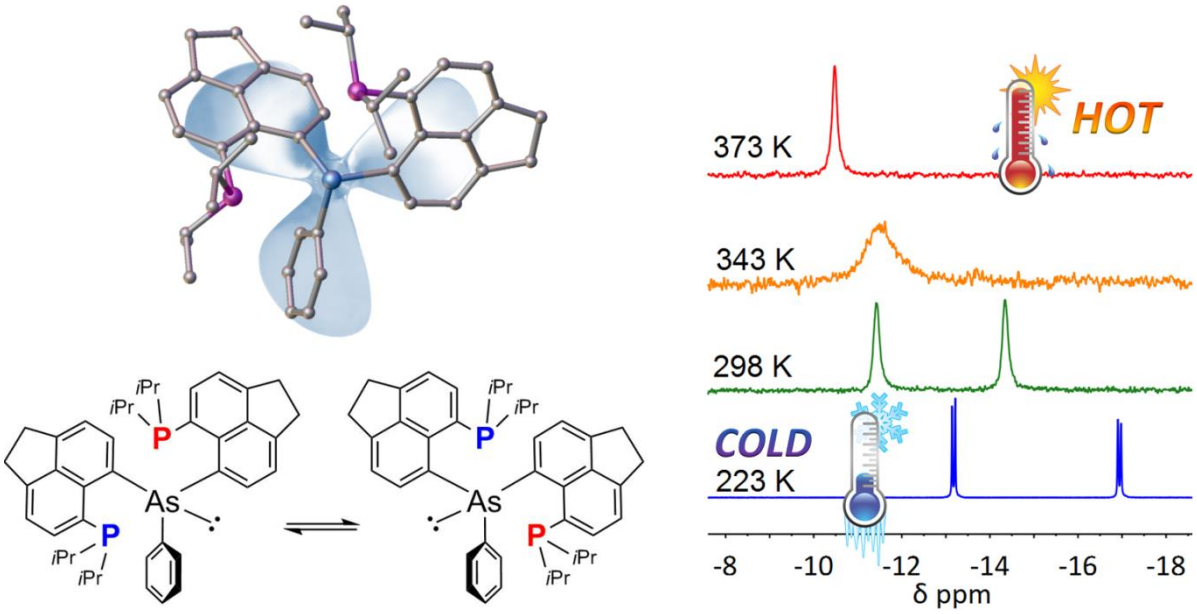

A series of propeller-shaped crowded bis and tris(peri-substituted) pnictogens has been synthesised and fully characterised, including single crystal X-ray diffraction. Remarkable $^{8TS}J_{PP}$ couplings of 11.5 and 25.8 Hz were observed that are likely to stem from a "double through-space" (n(P)···n(E)···n(P) (E = As, Sb) interaction, in which the central pnictogen's lone pair acts as a "relay" between the two magnetically inequivalent phosphorus nuclei.

References

(1) Broda, H.; Hinrichsen, S.; Tuczek, F. *Coord. Chem. Rev.* **2013**, *257*, 587.

(2) Pascariu, A.; Iliescu, S.; Popa, A.; Ilia, G. *J. Organomet. Chem.* **2009**, *694*, 3982.

(3) Hewertson, W.; Watson, H. R. *J. Chem. Soc.* **1962**, 1490.

(4) Hartley, J. G.; Venanzi, L. M.; Goodall, D. C. *J. Chem. Soc.* **1963**, 3930.

(5) Kyba, E. P.; Hudson, C. W.; McPhaul, M. J.; John, A. M. *J. Am. Chem. Soc.* **1977**, *99*, 8053.

(6) Jana, B.; Hovey, M.; Ellern, A.; Pestovsky, O.; Sadow, A. D.; Bakac, A. *Dalton Trans.* **2012**, *41*, 12781.

(7) Barney, A. A.; Fanwick, P. E.; Kubiak, C. P. *Organometallics* **1997**, *16*, 1793.

(8) Ray, M. J.; Randall, R. A. M.; Athukorala Arachchige, K. S.; Slawin, A. M. Z.; Bühl, M.; Lébl, T.; Kilian, P. *Inorg. Chem.* **2013**, *52*, 4346.

(9) Kilian, P.; Slawin, A. M. Z. *Dalton Trans.* **2007**, 3289.

(10) Yamashita, M.; Watanabe, K.; Yamamoto, Y.; Akiba, K. *Chem. Lett.* **2001**, 1104.

(11) Ritch, J. S.; Julienne, D.; Rybchinski, S. R.; Brockman, K. S.; Johnson, K. R. D.; Hayes, P. G. *Dalton Trans.* **2014**, *43*, 267.

(12) Wawrzyniak, P.; Fuller, A. L.; Slawin, A. M. Z.; Kilian, P. *Inorg. Chem.* **2009**, *48*, 2500.

(13) Adams, E.; Jeter, D.; Cordes, A. W.; Kolis, J. W. *Inorg. Chem.* **1990**, *29*, 1500.

(14) Herrmann, W. A.; Karsch, H. H. *Synthetic Methods of Organometallic and Inorganic Chemistry Vol 3: Phosphorus, Arsenic, Antimony and Bismuth*; Thieme: New York, 1996; Vol. 3.

(15) Chalmers, B. A.; Bühl, M.; Athukorala Arachchige, K. S.; Slawin, A. M. Z.; Kilian, P. *Chem. Eur. J.* **2015**, *21*, 7520.

(16) Batsanov, S. S. *Inorg. Mater.* **2001**, *37*, 871.

(17) Hierso, J.-C. *Chem. Rev.* **2014**, *114*, 4838.

(18) Reed, A. E.; Curtiss, L. A.; Weinhold, F. *Chem. Rev.* **1988**, *88*, 899.

(19) Note that empirical dispersion corrections are instrumental to reach this good agreement; at the standard B3LYP/6-31G* level, the P-As bond distances are significantly overestimated (e.g. mean value 3.306 A in 2.

(20) Wiberg, K. B. *Tetrahedron* **1968**, *24*, 1083.

(21) Nordheider, A.; Hupf, E.; Chalmers, B. A.; Knight, F. R.; Bühl, M.; Mebs, S.; Chęcińska, L.; Lork, E.; Camacho, P. S.; Ashbrook, S. E.; Athukorala Arachchige, K. S.; Cordes, D. B.; Slawin, A. M. Z.; Beckmann, J.; Woollins, J. D. *Inorg. Chem.* **2015**, *54*, 2435.

(22) Knight, F. R.; Diamond, L. M.; Athukorala Arachchige, K. S.; Sanz Camacho, P.; Randall, R. A. M.; Ashbrook, S. E.; Bühl, M.; Slawin, A. M. Z.; Woollins, J. D. *Chem. Eur. J.* **2015**, *21*, 3613.

(23) Armarego, W. L. F.; Chai, C. L. L. *Purification of Laboratory Chemicals (6th Edition)*; 6th ed.; Elsevier: Burlington.